

## X-RAY TRANSIENTS IN THE ADVANCED LIGO/VIRGO HORIZON

JONAH KANNER<sup>1,2</sup>, JOHN BAKER<sup>2</sup>, LINDY BLACKBURN<sup>2</sup>, JORDAN CAMP<sup>2</sup>, KUNAL MOOLEY<sup>3</sup>,  
RICHARD MUSHOTZKY<sup>4,5</sup>, AND ANDY PTAK<sup>4</sup>

<sup>1</sup> LIGO-California Institute of Technology, Pasadena, CA 91125, USA; [jonah.kanner@ligo.org](mailto:jonah.kanner@ligo.org)

<sup>2</sup> NASA Goddard Space Flight Center, Mail Code 663, Greenbelt, MD 20771, USA

<sup>3</sup> California Institute of Technology, Astronomy Department, Mail Code 249-17, Pasadena, CA 91125, USA

<sup>4</sup> NASA Goddard Space Flight Center, Mail Code 661, Greenbelt, MD 20771, USA

<sup>5</sup> Astronomy Department, University of Maryland, College Park, MD 20742, USA

Received 2013 May 13; accepted 2013 July 12; published 2013 August 16

### ABSTRACT

Advanced LIGO and Advanced Virgo will be all-sky monitors for merging compact objects within a few hundred megaparsecs. Finding the electromagnetic counterparts to these events will require an understanding of the transient sky at low redshift ( $z < 0.1$ ). We performed a systematic search for extragalactic, low redshift, transient events in the *XMM-Newton* Slew Survey. In a flux limited sample, we found that highly variable objects comprised 10% of the sample, and that of these, 10% were spatially coincident with cataloged optical galaxies. This led to  $4 \times 10^{-4}$  transients per square degree above a flux threshold of  $3 \times 10^{-12}$  erg cm<sup>-2</sup> s<sup>-1</sup> (0.2–2 keV) which might be confused with LIGO/Virgo counterparts. This represents the first extragalactic measurement of the soft X-ray transient rate within the Advanced LIGO/Virgo horizon. Our search revealed six objects that were spatially coincident with previously cataloged galaxies, lacked evidence for optical active galactic nuclei, displayed high luminosities  $\sim 10^{43}$  erg s<sup>-1</sup>, and varied in flux by more than a factor of 10 when compared with the *ROSAT* All-Sky Survey. At least four of these displayed properties consistent with previously observed tidal disruption events.

**Key words:** galaxies: nuclei – gravitational waves – surveys – X-rays: general

**Online-only material:** color figures

### 1. INTRODUCTION

The X-ray band provides an opportunity to find high confidence counterparts to the compact object mergers that will be discovered with the second generation LIGO and Virgo gravitational wave detectors. Within this decade Advanced LIGO (Harry et al. 2010) and Advanced Virgo<sup>6</sup> (Acernese et al. 2008) are expected to begin detecting mergers of binary neutron stars and neutron stars with stellar mass black holes out to distances of a few hundred megaparsecs (Abadie et al. 2010). Placing these mergers in an astrophysical context and maximizing the scientific returns will require finding electromagnetic counterparts to the events (Bloom et al. 2009; Phinney 2009). However, the positional accuracy of the gravitational wave detectors will be limited to tens or hundreds of square degrees (Abadie et al. 2012; Fairhurst 2009; Klimenko et al. 2011; Nissanke et al. 2013). Thus, associating an electromagnetic counterpart with a LIGO/Virgo detection will require an understanding that a chance coincidence within the LIGO/Virgo horizon is unlikely, even within a large sky region. In the optical band, large area survey instruments such as Pan-STARRS, Palomar Transient Factory, SkyMapper, and the future LSST will have a daunting challenge separating LIGO counterparts from stellar variability, supernovae, and other confusion sources (Kulkarni & Kasliwal 2009; Nissanke et al. 2013), but may leverage the large ongoing effort to create schemes of automated or semi-automated transient classification (e.g., Bloom et al. 2012). The radio band may also be searched for counterparts to GW events (Predoi et al. 2010; Lazio et al. 2012), and large area searches for radio transients are rapidly developing (Stappers et al. 2011; Bhat et al. 2013).

In the X-ray band, low number counts at bright flux levels may make identification of a LIGO/Virgo counterpart more

straightforward. However, studies of X-ray variability have tended to focus on persistent or repeating sources, particularly active galactic nucleus (AGN), X-ray binaries, or stellar flares. Past all-sky searches for soft X-ray transients include searches in the *ROSAT* All-Sky Survey (RASS) data (Greiner et al. 2000a; Fuhrmeister & Schmitt 2003), work with the *XMM-Newton* Slew Survey (Esquej et al. 2007; Starling et al. 2011), and searches for flashes lasting a few seconds (Gotthelf et al. 1996; Connors et al. 1986).

A small fraction of compact object mergers are thought to create short gamma-ray bursts (GRBs; e.g., Fox et al. 2005; Eichler et al. 1989), and if one occurred within the Advanced LIGO/Virgo horizon, the X-ray afterglow could be bright ( $\sim 10^{-12}$  erg cm<sup>-2</sup> s<sup>-1</sup>) for about a day after the merger (Kanner et al. 2012). Short GRBs may be associated with mergers of two neutron stars, or a neutron star with a black hole, and are typically characterized by a prompt emission lasting less than 2 s, and a spectrum that is somewhat harder than the more prevalent “long GRBs” associated with stellar core collapse (Nakar 2007). Some double neutron star mergers may also exhibit a bright X-ray counterpart due to emission from a magnetar-powered ejecta (Gao et al. 2013; Zhang 2013; Metzger et al. 2008), observable for up to a few thousand seconds after the merger. Such signals could be detectable with a wide field focusing instrument such as the proposed ISS-Lobster (Camp et al. 2013) or A-STAR (Osborne et al. 2013), or in some cases with multiple observations of *Swift*/XRT (Kanner et al. 2012; Evans et al. 2012). In order to estimate the ability to identify a unique source in such a campaign, we have searched the *XMM-Newton* Slew Survey Clean Source Catalog, version 1.5 (XMMSL1; Saxton et al. (2008)) for objects consistent with counterparts to compact object mergers observable with the future Advanced LIGO and Advanced Virgo observatories. We sought both to measure the density of such events that are observable in a given moment and to characterize the nature

<sup>6</sup> <https://tds.ego-gw.it/itf/tds/file.php?callFile=VIR-0027A-09.pdf>

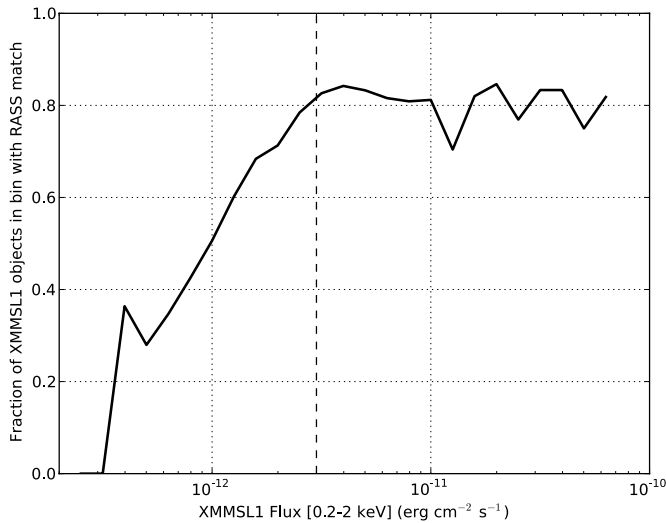


**Figure 1.** The fraction of XMMSL1 objects listed with RASS matches in each flux bin. The vertical line indicates the flux limit selected for the search.

of the objects we found. Our search criteria emphasized low redshift, transient objects, and were similar to those of Esquej et al. (2007). However, this study used a data set covering five times the slew survey area available in 2007 and included a systematic measurement of the transient density using a simple, easy to emulate definition.

## 2. CANDIDATE SELECTION

We designed our selection criteria to seek objects consistent with a transient event within the Advanced LIGO/Virgo neutron star merger horizon distance. We used the XMMSL1 soft band of 0.2–2 keV for all flux measurements, since it is similar to the *ROSAT* PSPC band. The XMMSL1 includes identifications with RASS sources with a 30'' search radius (Voges et al. 1999; Saxton et al. 2008). We found that 80% of XMMSL1 sources brighter than  $3 \times 10^{-12} \text{ erg s}^{-1} \text{ cm}^{-2}$  had matches in the RASS with no improvement in overlap for brighter sources, so we took this as the flux limit for our search (see Figure 1). For each XMMSL1 object brighter than this threshold, we attempted to place a flux upper-limit in the RASS data set. We explored a range of different radii for the source extraction region using data corresponding to *ROSAT* detected sources, and found that a 205'' radius was needed to recover the median source with 90% of the expected flux. For the XMMSL1 objects above our flux threshold, Bayesian upper-limits corresponding to a  $2\sigma$  confidence level were applied to the *ROSAT* PSPC counts found within a 205'' extraction radius. To convert from counts to flux in the 0.2–2 keV band, we used webPIMMS<sup>7</sup> with the same source assumptions that were used in the XMMSL1, namely, a power-law spectra with an index of 1.7 and a hydrogen column density of  $3 \times 10^{20} \text{ cm}^{-2}$ . For each object, we took a ratio between XMMSL1 flux as listed in the catalog and the RASS upper-limit we constructed, and kept only objects with a flux ratio greater than 10 (see Figure 2). These objects, or any objects with a flux ratio greater than 10, are referred to as “transients” for the rest of this paper. Since we were interested only in extragalactic objects within a few hundred megaparsecs, we expected their host galaxies to be visible in large optical and near infrared surveys such as the Sloan Digital Sky Survey<sup>8</sup> (SDSS) and

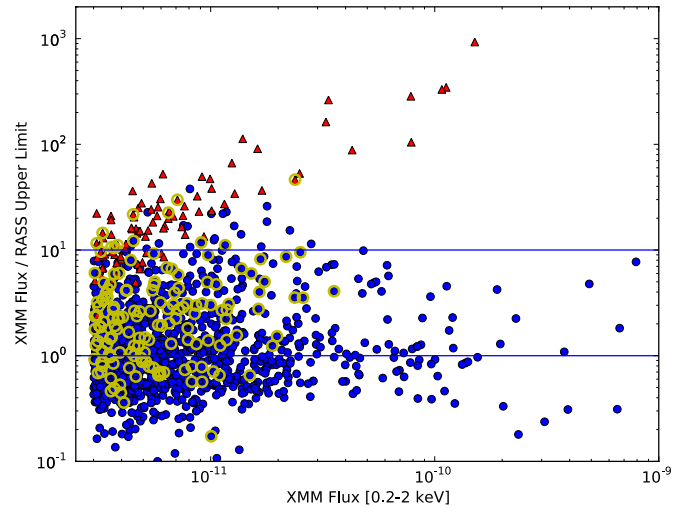


**Figure 2.** Sources above our flux threshold in the XMMSL1. The y-axis represents the flux ratio between the XMMSL1 and RASS. All RASS fluxes are calculated as  $2\sigma$  upper limits, with red triangles indicating a number of RASS counts consistent with a non-detection at the  $2\sigma$  level, and blue circles indicating a source was detected. A yellow, hollow circle indicates an identification with a galaxy in the XMMSL1.

(A color version of this figure is available in the online journal.)

the Two Micron All Sky Survey. Therefore, we demanded that candidates be listed in XMMSL1 as spatially coincident with a known galaxy or galaxy cluster with a 30'' match radius. Finally, we checked our candidates for an AGN association, and for any other observations in the HEASARC database.<sup>9</sup>

## 3. RESULTS

### 3.1. A Snapshot of the Sky

Our search showed that source variability seemed to naturally divide the XMMSL1 survey into two classes (see Figure 2). The first class, representing roughly 90% of sources, was mainly below the flux ratio threshold value of 10, and mainly detected in both the RASS and the XMMSL1, indicated by blue circles in the figure. The distribution of sources detected in both XMMSL1 and the RASS is shown in Figure 3, and is loosely consistent with a logarithmic distribution. Their flux ratios have a logarithmic standard deviation corresponding to a flux ratio of 2.5, and a flux ratio of more than 10 corresponds to a  $2.5\sigma$  level of variability. We label this class “continuum variability” and note that the variability arises from a wide range of causes, including most AGN variability, measurement errors, and differences in the spectral response of the two instruments.

A different, more dramatic, type of variability was also present in the survey. At high flux values (toward the right in Figure 2), there is a clear separation between the sources which were observed in the RASS, and those which were not observed in the RASS. The ratios between the XMMSL1 flux and the RASS upper limit for sources not detected in RASS are plotted as red triangles in the figure. This second population (state-change objects) represents sources which were in some distinctly different state at the time of the RASS and XMMSL1 observations. Known examples in this class include X-ray binaries in different states, flaring stars, tidal disruption events (TDEs), and classical novae. This class could be defined as sources with a flux and flux ratio which places

<sup>7</sup> <http://heasarc.gsfc.nasa.gov/Tools/w3pimms.html>

<sup>8</sup> <http://www.sdss.org>

<sup>9</sup> <http://heasarc.gsfc.nasa.gov/>

**Table 1**  
The List of Transient Objects with Galaxy Associations Found in our Search

Name	Flux (cgs)	Ratio	$D_L^a$ (Mpc)	Luminosity (erg s $^{-1}$ )	Notes	Date
XMMSL1...						
J202320.7–670021	$2.3 \times 10^{-11}$	46	67	$1.2 \times 10^{43}$	Not AGN <sup>c</sup>	2009 Oct 05
J084837.9+193527	$6.4 \times 10^{-12}$	23	283	$6.1 \times 10^{43}$	Emission line galaxy <sup>d</sup>	2010 Oct 17
J182609.9+545005	$4.5 \times 10^{-12}$	22	650	$2.2 \times 10^{44}$	Not AGN	2005 Nov 01
J152408.6+705533	$3.3 \times 10^{-12}$	15	256	$2.6 \times 10^{43}$	Spiral galaxy	2006 Jan 24, 2007 Nov 01
J202554.8–511629	$9.1 \times 10^{-12}$	12	?	?		2010 Apr 16
J131951.9+225957	$3.7 \times 10^{-12}$	10	99	$4.3 \times 10^{42}$	Not AGN <sup>d</sup>	2005 Jul 15
J111527.3+180638	$7.1 \times 10^{-12}$	30	12	$1.2 \times 10^{41}$	Esquej.	2003 Nov 22
J155631.5+632540	$3.8 \times 10^{-12}$	21	?	?	Bad match	2010 Jun 23
J020303.1–074154	$3.1 \times 10^{-12}$	12	272	$2.7 \times 10^{43}$	Esquej.	2004 Jan 14
J170543.0+850523	$4.5 \times 10^{-12}$	12	?	?	Cluster	2008 Aug 31
J013727.9–195605	$1.2 \times 10^{-11}$	11	1320	$2.1 \times 10^{45}$	Cluster	2007 Dec 27
J104745.6–375932	$3.6 \times 10^{-12}$	10	335	$4.8 \times 10^{43}$	AGN <sup>c</sup>	2003 Dec 14

**Notes.** The listed fluxes are those reported in XMMSL1 catalog (Saxton et al. 2008). The column labeled “Ratio” shows the ratio between the observed XMMSL1 flux and a  $2\sigma$  upper limit based on the corresponding RASS data. Each distance ( $D_L$ ) and inferred luminosity is based on the overlap of the  $2\sigma$  XMMSL1 position with an optically identified galaxy. The note “Not AGN” signals that an available spectra shows no evidence for AGN emission. The objects with the note Esquej were reported as tidal disruption event candidates by Esquej et al. (2007). Bad match denotes that the matched galaxy was separated from the XMMSL1 source by more than the  $2\sigma$  position uncertainty. The six objects above the horizontal line are further discussed in Section 3.

<sup>a</sup> The luminosity distance of the associated galaxy.

<sup>b</sup> Based on inspection of 6dF spectrum.

<sup>c</sup> Based on inspection of SDSS spectrum.

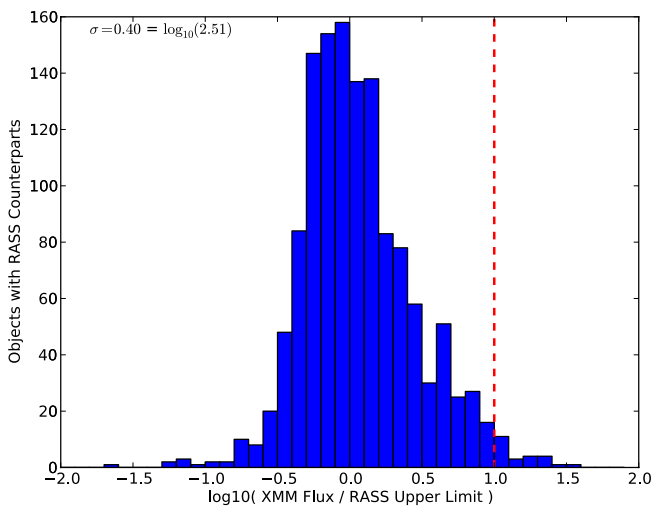


**Figure 3.** Histogram of the logarithm of the flux ratio for objects detected in both XMMSL1 and RASS. The standard deviation of the distribution is 0.40, corresponding to a flux ratio of 2.51. By this measure, then, a threshold on the flux ratio of 10 requires an object’s variability to be beyond  $2.5\sigma$  in the distribution.

(A color version of this figure is available in the online journal.)

them outside the distribution of continuum variability shown in Figure 3. Many of the sources with RASS non-detections (red triangles) seem to belong to this class. Though the separation between the RASS detections and non-detections in Figure 2 disappears at low flux values, the vertical placement of the non-detections is determined primarily by the limiting flux of the RASS observation. Therefore, any of the non-detections would potentially sit higher in this plane with data from a deeper observation. Given that some of the bright XMMSL1 sources were seen to vary by more than a factor of 100, it would be surprising if this was not also the case for some of the dimmer sources as well.

Some of the state-change objects observed in XMMSL1 were also studied by Starling et al. (2011). In their study, the authors

selected 97 sources from v1.4 of the *XMM-Newton* Slew Survey with no identified optical or RASS counterpart. They then collected pointed observations for 94 of these with *Swift*/XRT in an attempt to classify them. In their paper, Starling et al. (2011) report that 71% of the targets were not seen in the *Swift* observations, implying they had faded by at least a factor of 10. The isotropic distribution and lack of an optical counterpart of these mysterious sources led the authors to conclude that they represented a primarily extragalactic population. None of the sources in the Starling study appeared in our final candidate list, as the former campaign required sources to have no optical counterpart, where we required a match to a known optical galaxy. However, if the bulk of the transients studied by Starling et al. were extragalactic, as they concluded, then the objects listed in Table 1 may represent low redshift objects from the same population. In particular, the study found 47 objects detected in the *XMM-Newton* soft band, but not detected with *Swift*.

We wished to use the variability in this data set to characterize the chance of a spurious detection in coincidence with a trigger from the future advanced LIGO/Virgo network. We applied the selection criteria described in Section 2, and the statistical results of our search are presented in Figure 4. Each curve in the figure shows the density of sources in the set with fluxes above the value on the X-axis. The top curve (black, dotted) is the log  $N$ –log  $S$  curve of the XMMSL1 catalog, assuming 32,800 deg $^2$  of coverage. The bottom curve (blue, solid) is the result of our search criteria, which resulted in 12 transient objects spatially coincident with a known galaxy (see Table 1, yellow circles in Figure 2). In requiring the galaxy association, we included associations with both galaxies and galaxy clusters, but rejected associations labeled in the XMMSL1 as AGN (Seyfert, BL Lac, etc.).

Most of the matched host galaxies with available redshifts were located at luminosity distances of less than 350 Mpc. This is most likely because available catalogs of galaxies were dominated by relatively shallow observations from large area surveys. Kasliwal (2011) found that current galaxy databases

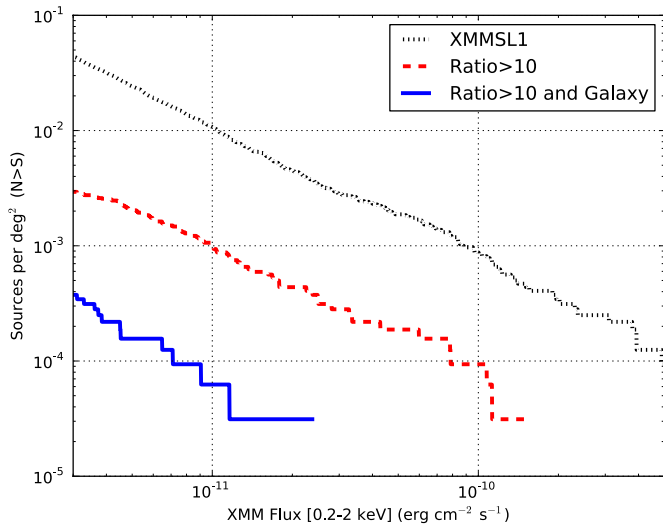


**Figure 4.** The statistical result of our search for low-redshift transients. The top curve (black) shows the  $\log N$ - $\log S$  plot for the XMMSL1 catalog, containing 1411 objects above our flux threshold. The second curve (red) shows the distribution of the 97 transients, defined as at least 10 times brighter in XMMSL1 than in RASS. The bottom curve includes only transient objects that are spatially coincident with a known galaxy, after rejecting previously identified AGNs.

(A color version of this figure is available in the online journal.)

(NED,<sup>10</sup> HyperLeda,<sup>11</sup> etc.) were 50% complete to 200 Mpc, with a steep downward trend in completeness as a function of distance. This distance scale was well aligned with the reach of Advanced LIGO and Virgo, which will detect NS–NS mergers primarily between 100 and 400 Mpc (Nissanke et al. 2013). From an operational perspective, then, future searches for X-ray counterparts to LIGO/Virgo transients may not need to obtain a redshift estimate for each possible host galaxy in the field; any galaxy bright enough to be cataloged by a large area survey without an AGN signature is likely to be within the Advanced LIGO horizon. For our interpretation, we have taken this approach. This would tend to skew our estimates of unrelated counterparts to be artificially high, because using the estimated distance to the gravitational wave source can be a powerful tool for rejecting potential host galaxies at inconsistent redshifts (Nissanke et al. 2013).

To interpret Figure 4, we note that typical exposures in the *XMM-Newton* Slew Survey were 5–20 s, so we assumed that the transients that passed our selection criteria were of longer duration than the *XMM-Newton* exposures. Though the Slew Survey was not uniform in any sense, the coverage area was largely random, and so we assumed that the density of sources which passed our cuts was not strongly biased by target selection. The survey did include some repeat visits, and only covered 20,900 unique square degrees. However, the time between repeated visits was typically  $>1$  yr, which was more than the expected timescale for fading of X-ray counterparts to neutron star mergers. For this reason, we interpreted our results based on 32,800  $\text{deg}^2$  of coverage, noting that this choice leads to at most a 60% systematic in our results. So, for example, the 12 sources above our flux threshold may be interpreted as  $4 \times 10^{-4}$  transients per square degree on timescales shorter than the  $\sim 15$  yr between RASS and XMMSL1.

The positional uncertainties associated with a trigger from the LIGO/Virgo network are expected to vary a great deal

depending on signal-to-noise ratio and other factors; however, studies typically quote numbers between 20 and 200  $\text{deg}^2$  for the position uncertainty of a low signal-to-noise ratio trigger with three sensitive gravitational wave detectors operational (Abadie et al. 2012; Fairhurst 2009; Klimentenko et al. 2011). Searching such a large area for an X-ray counterpart will require a relatively high flux limit to the search, since the instrument will have to either be very wide field or will have to use short exposures for many tiles. For example, in principle *Swift*/XRT could utilize  $\sim 100$  s exposures to tile as much as 35  $\text{deg}^2$  in a day, though only to a depth of  $6 \times 10^{-12} \text{ erg cm}^{-2} \text{ s}^{-1}$  (Kanner et al. 2012). While practical issues concerned with many repointings of the instrument may make this difficult in practice, Figure 4 shows that there would be less than a 1% chance of finding a transient in this search area by chance. A more natural scenario would be the application of a very wide-field, focusing instrument such as the proposed ISS-Lobster. The proposed instrument would image a 400  $\text{deg}^2$  field of view to a depth of around  $10^{-11} \text{ erg s}^{-1} \text{ cm}^{-2}$  in a 20 minute exposure. Applying these numbers, this observation would have a 3% chance of imaging an unrelated transient coincident with a known host galaxy, or less than a 1% chance if we imagine only using the fraction of the field that overlaps the LIGO/Virgo errorbox. Similar considerations would apply to other wide field-of-view instruments, including MAXI (Matsuoka et al. 2009) or the proposed A-STAR (Osborne et al. 2013).

Of course, the details of how a future search is carried out would have a strong influence on these numbers. Choosing to define a transient as an object that brightens by at least a factor of 10 is somewhat arbitrary, though for our data set, the naturally distinct classes of continuum variability and state-change variability seen in Figure 2 appears to somewhat justify this choice. Another important factor is the completeness of the galaxy catalog, which is likely to evolve rapidly due to efforts by several large area surveys (Metzger et al. 2013). On the other hand, at the order-of-magnitude level, these results seem to be robust. The associations of these sources with the host galaxies do not appear to be spurious (See Section 4.5), so adjusting the match radius used to associate host galaxies and sources will make little impact. Similarly, increasing the searched area around the host galaxy due to “kicks” in the binary (Fryer & Kalogera 1997) will not change these statistics substantially. A variety of models, with some validation from studies of short GRB host galaxies, have concluded that the majority of NS–NS mergers occur within 10 or a few tens of kiloparsecs from the centers of their host galaxies (Berger 2010; Brandt & Podsiadlowski 1995; Bloom et al. 1999; Fryer et al. 1999; Belczynski et al. 2006). At 200 Mpc, the 30'' search radius used for galaxy association corresponds to an offset from the host galaxy of 30 kpc. Berger (2010) showed that for a range of models, this search radius would include 70%–90% of NS–NS mergers. On the other hand, models do exist with more extreme kick velocities, leading to mergers that occur up to a megaparsec away from the host galaxy (Kelley et al. 2010). To accommodate these models would mean using a somewhat larger search radius, and so the requirement of a galaxy association may become less useful. Additional surveys could increase the number of known galaxies, and so increase false associations by a factor of  $\sim 2$  or more. However, eliminating possible hosts with redshifts inconsistent with the GW data could limit this effect (Nissanke et al. 2013).

Finally, we note that the separation of soft X-ray sources into state-change transients and continuum variability appears to

<sup>10</sup> <http://ned.ipac.caltech.edu/>

<sup>11</sup> <http://leda.univ-lyon1.fr/>



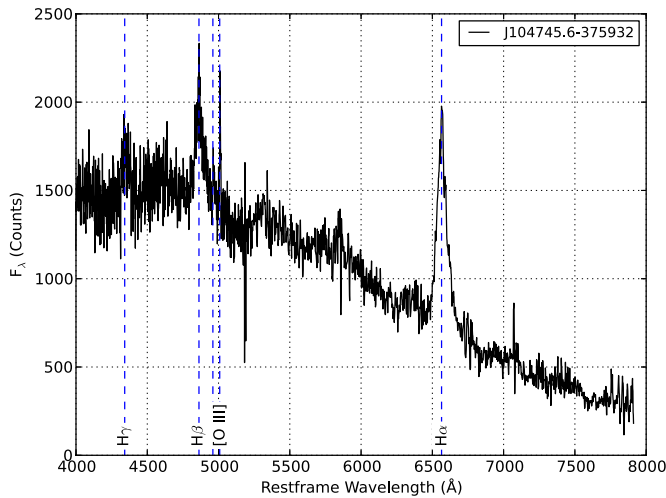


**Figure 5.** Optical spectrum of the host galaxy matched to XMMSL1 J104745.6–375932 obtained by the 6dF survey, plotted in the restframe using a redshift of 0.075. The strong, broad hydrogen lines and the blue spectrum are characteristic of quasars.

(A color version of this figure is available in the online journal.)

occur naturally. For these reasons, we expect that the finding that around 10% of bright, soft X-ray sources demonstrate a state-change brightening over long timescales, and that around 10% of these can be associated with galaxies within 200 Mpc, will prove true for future searches with perhaps a factor of a few uncertainty in both cases. For searches for X-ray counterparts to advanced LIGO/Virgo triggers, this criteria represents a two order of magnitude reduction in the background rate, as compared with the density of X-ray sources on the sky which has been used to estimate the density of spurious associations in past work (Evans et al. 2012).

### 3.2. Further Selection

After identifying our list of 12 candidates, we sought to characterize them as far as possible. We inspected optical images of the host galaxies and searched for additional data using the HEASARC database. We also inspected publicly available and newly obtained optical spectra to check for AGN signatures. Two of the objects were rediscoveries of previously published candidate TDEs (XMMSL1 J020303.1–074154 and XMMSL1 J111527.3+180638; Esquej et al. 2007). One object showed broad AGN emission lines in a 6dF<sup>12</sup> archived spectrum, and was seen in XRT data to have an X-ray spectrum consistent with an AGN (XMMSL1 J104745.6–375932; see Figure 5). One object’s (XMMSL1 J155631.5+632540)  $2\sigma$  position circle did not include the matched host galaxy. Two of the sources (XMMSL1 J013727.9–195605 and XMMSL1 J170543.0+850523) were matched to galaxy clusters with ambiguous galaxy associations.

This left six objects which exhibited some interesting properties. Of the five where we obtained a redshift (either through observations or the literature), most corresponded to luminosities distances less than 300 Mpc in a standard cosmology; the furthest was placed around 650 Mpc. We examined optical spectra for five of the host galaxies, and none of these showed broad emission lines, though two (XMMSL1 J084837.9+193527 and J152408.6+705533) showed narrow emission lines (see Figures 6–10). They were all soft sources, and only one has a measured hardness ratio presented in XMMSL1 (XMMSL1

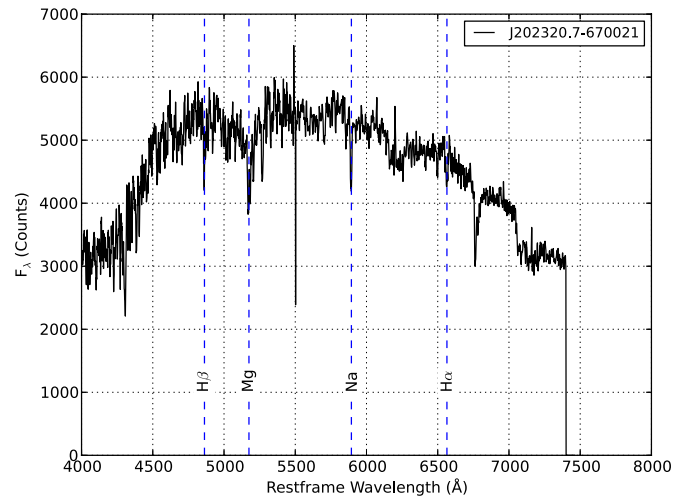


**Figure 6.** Optical spectrum of the host galaxy matched to XMMSL1 J202320.7–670021, obtained by the 6dF survey, and plotted in the restframe using a redshift of  $z = 0.016$ . The galaxy is dominated by stellar absorption features.

(A color version of this figure is available in the online journal.)

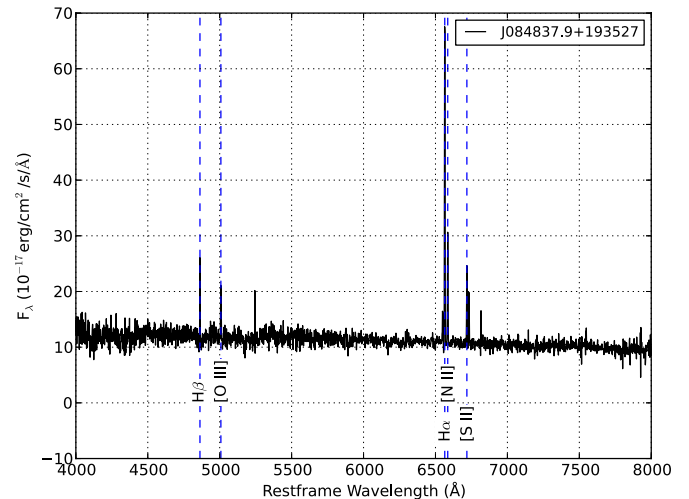


**Figure 7.** Optical spectrum of the host galaxy matched to XMMSL1 J084837.9+193527, obtained by the SDSS, plotted in the rest frame using a redshift of 0.064. A test using diagnostic narrow line ratios shows this to be a star forming galaxy, as described in the text.

(A color version of this figure is available in the online journal.)

J182609.9+545005:  $-0.46$ ). We searched HEASARC for observations with *Chandra*, *Swift*, and *XMM-Newton*, but found no observations containing any of the six remaining sources. These six objects were generally extragalactic, more powerful than  $4 \times 10^{42}$  erg s<sup>-1</sup>, close ( $D_L < 300$  Mpc), variable by at least  $10\times$ , and lacking evidence for AGN activity. This makes them difficult to characterize, as well as energetic and variable. In the next section, we discuss possible characterizations for these sources, and attempt to address the likelihood of each.

## 4. POSSIBLE CHARACTERIZATIONS

### 4.1. Tidal Disruption Events

TDEs are thought to occur at a rate of  $\sim 10^{-5}$  yr<sup>-1</sup> Mpc<sup>-3</sup> and display initial luminosities up to  $\sim 10^{45}$  erg s<sup>-1</sup> during the first few days or weeks followed by a characteristic dimming  $\propto t^{-5/3}$  (Bade et al. 1996; Wang & Merritt 2004). Under these

<sup>12</sup> <http://www.aao.gov.au/6dFGS>

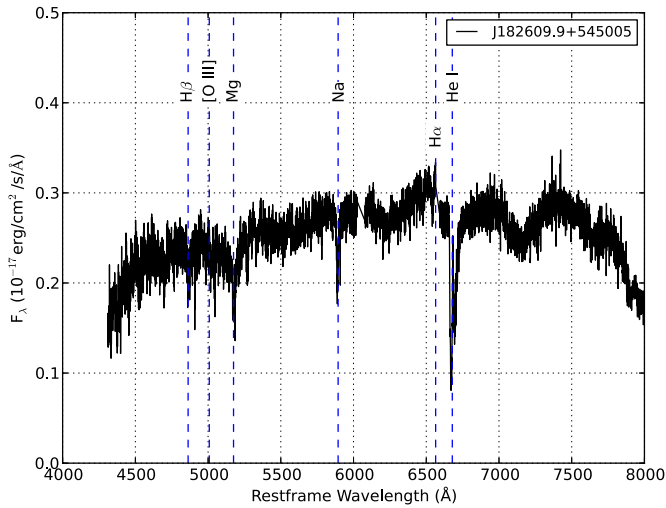


**Figure 8.** Optical spectrum of the host galaxy matched to XMMSL1 J182609.9+545005, obtained with the Keck/DEIMOS on 2013 May 3, plotted in the rest frame with a redshift of 0.14. The absence of emission lines and red color suggest this is a red galaxy without an active central region.

(A color version of this figure is available in the online journal.)

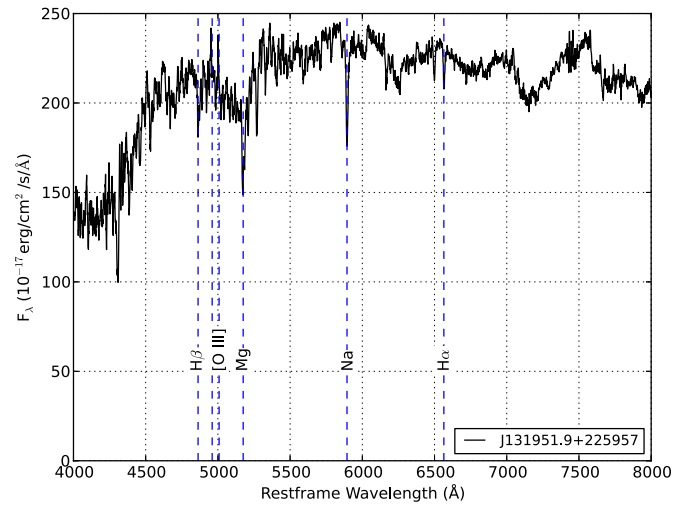


**Figure 10.** Optical spectrum of the host galaxy matched to XMMSL1 J131951.9+225957, obtained by the SDSS, plotted in the rest frame with a redshift of 0.023. The spectrum appears to be dominated by stellar absorption features.

(A color version of this figure is available in the online journal.)

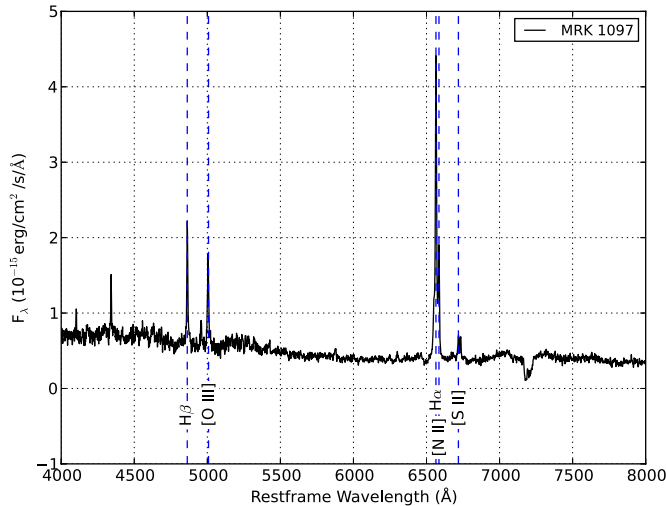


**Figure 9.** Optical spectrum of the host galaxy matched to XMMSL1 J152408.6+705533, obtained on 2013 April 15 with the 200 inch Hale Telescope at Palomar Observatory, plotted in the rest frame with a redshift of 0.059. The narrow line features and *WISE* colors suggest this is a spiral galaxy, and so is unlikely to host an active nucleus.

(A color version of this figure is available in the online journal.)

assumptions, at 200 Mpc, such an event would be visible for a few months to years above a flux of  $3 \times 10^{-12} \text{ erg s}^{-1} \text{ cm}^{-2}$ . A number of TDE candidates have been discovered through their X-ray emission (Komossa & Bade 1999; Grupe et al. 1999; Komossa & Greiner 1999; Greiner et al. 2000b; Maksym et al. 2010; Lin et al. 2011). In addition, there have been discoveries made using ultraviolet surveys, such as those discussed in Gezari et al. (2006, 2012), and with optical surveys (van Velzen et al. 2011; Drake et al. 2011). There have also been two well-studied TDEs discovered with the *Swift* satellite (e.g., Bloom et al. 2011; Levan et al. 2011; Burrows et al. 2011; Cenko et al. 2012).

In fact, some TDEs have already been discovered using data from the *XMM-Newton* Slew Survey. Last year, Saxton et al. (2012) reported on the discovery of an X-ray flare in SDSS J120136.02+300305.5 found in data from the *XMM-Newton* Slew Survey, and followed up with pointed observations of

**Table 2**  
Galaxy Matches from the XMMSL1 Catalog for Six Transients  
Identified by our Search

Name XMMSL1...	Galaxy Match	Offset (arcsec)
J202320.7–670021	6dFGS gJ202322.7–670046	$27 \pm 13$
J084837.9+193527	SDSS J084838.57+193528.9	$10 \pm 22$
J182609.9+545005	2MASX J18261094+5450052	$7 \pm 5$
J152408.6+705533	MRK 1097	$1 \pm 3$
J202554.8–511629	2MASX J20255579–5116276	$9 \pm 19$
J131951.9+225957	NGC 5092	$4 \pm 2$

**Notes.** The offset shows the angular distance between the galaxy and the source position, along with the uncertainty quoted in the catalog.

*Swift*/XRT. Their program is designed to find flaring X-ray events soon after they begin to enable prompt follow-up. The flux of the corresponding observation listed in the XMMSL1 was below our flux threshold, so this event was not rediscovered by our search. Esquej et al. (2007, 2008) found two TDEs in the *XMM-Newton* Slew Survey, including one TDE above our flux threshold (see Table 1), via a search with similar selection criteria, but using the first release (v1.1) of the XMMSL1 catalog, covering  $6300 \text{ deg}^2$ . Our search used the latest release (v1.5) of XMMSL1, covering  $32,800 \text{ deg}^2$  ( $20,900 \text{ deg}^2$  of unique area). This suggests that we should expect around four new TDEs in our data set. Given the lack of nuclear activity in some of the host galaxies, the high luminosity of the sources, and the positions which are consistent with the center of the host galaxies, we expect this model will account for at least some of our candidates. For example, XMMSL1 J131951.9+225957 was matched to NGC 5092 with an offset from the center of the galaxy of only  $4''$ , compared with the match radius of  $30''$ , or the average XMMSL1 uncertainty of  $8''$  (see Table 2). An SDSS spectrum of this galaxy, shown in Figure 10, reveals only absorption features, making an AGN association unlikely. These features were consistent with a TDE description. The galaxy SDSS J084838.57+193528.9 showed some narrow emission line features. To characterize it, we used the best fit line profiles provided by the SDSS Science Archive Server. We found the

[N II]  $\lambda 6583/H\alpha$  ratio to be 0.32, and the [O III]  $\lambda 5007/H\beta$  ratio to be 0.67, so that this galaxy appeared to have a star-forming region, but no nuclear activity (Veilleux & Osterbrock 1987). For this reason, the observed variability in this galaxy also appeared consistent with a tidal disruption model. We obtained a spectrum of the host galaxy matched to XMMSL1 J182609.9+545005 on 2013 May 3, using the Keck/DEIMOS (Figure 8). The spectrum was dominated by absorption features, and showed no evidence for an active central region. The redshift we obtained ( $z = 0.14$ ) places this galaxy outside the planned Advanced LIGO horizon.

Finally, one object that passed our cuts, XMMSL1 J152408.6+705533, was observed twice in the XMMSL1, in 2006 January and 2007 November. In the 23 months between the observations, the source faded by a factor of three. Fitting a TDE light curve to these two points resulted in an event with starting time in 2004 March, and a luminosity of  $5.7 \times 10^{43} \text{ erg s}^{-1}$  1 yr after the start time. The implied energies were roughly consistent with previously observed TDEs (Esquej et al. 2008). We obtained a spectrum of the host galaxy, MRK 1097, with the 200 inch telescope at Palomar observatory, and found primarily narrow line emission features (see Figure 9). The *WISE* colors for this galaxy ( $[W1 - W2] = 0.3 \text{ mag}$  and  $[W2 - W3] = 1.8 \text{ mag}$ ) (Wright et al. 2010) and narrow line features suggested this is a spiral galaxy, and so is unlikely to host an AGN.

#### 4.2. GRB Afterglows

Short GRBs have been observed with a rate density of  $5\text{--}13 \text{ Gpc}^{-3} \text{ yr}^{-1}$ , implying a rate of around one per year within 300 Mpc (Nakar 2007; Coward et al. 2012). Long GRBs are observed with a rate density of  $0.5 \text{ Gpc}^{-3} \text{ yr}^{-1}$  (Nakar 2007), or one event every 20 yr within 300 Mpc. GRBs are known to display bright afterglows, typically observable in soft X-rays for a few hours up to a few days after the burst. However, most GRBs are observed much further away than 300 Mpc, so a burst at the distance of our objects would have an afterglow that would appear brighter, and would potentially be observable longer. Taking an optimistic but plausible scenario, a short GRB afterglow at the distances our objects, showing power-law dimming with a temporal index of 1.2, would display the flux levels observed with *XMM-Newton* 10–100 days after the burst. A model that includes a jet break would show a faster fading, with a temporal index closer to 2.0 (Racusin et al. 2009). This means that, even in the optimistic case, we might only expect one GRB per year within our search volume, and that a GRB’s afterglow would only be observable for one to three months. Based on these numbers, we believe there is less than a  $\sim 10\%$  chance that our candidate list, after the requirement of a galaxy association, includes one or more GRB afterglows.

On the other hand, there are related classes of transients, both observed and theoretical, that are thought to be more common in the local universe. Low-luminosity GRBs have been observed with a local rate density much higher than the rate of cosmologically observed bright GRBs (Soderberg et al. 2006; Cobb et al. 2006; Chapman et al. 2007). These events can have X-ray band afterglows that are less luminous than cosmological GRB afterglows, but otherwise with similar properties (Soderberg et al. 2006). So-called orphan afterglows and failed GRBs may also be more common in the local universe than the more commonly observed cosmological GRBs (Rhoads 2003; Huang et al. 2002), an idea that may be supported by a recent observation (Cenko et al. 2013). It is difficult to rule out the possibility that such an event is in our sample.

#### 4.3. Ultra-luminous X-ray Source

Ultra-luminous X-ray sources (ULXs) have been observed in several nearby galaxies, with X-ray luminosities of  $10^{38}\text{--}10^{41} \text{ erg s}^{-1}$ . These objects are known to exhibit short time variability, and have been observed in both high and low energy states (Winter et al. 2006). However, the luminosities of our sources exceed the range of known ULXs, so, these objects cannot be naturally characterized as ULXs, or at best, they would represent extreme examples of the class.

#### 4.4. AGN

We inspected optical spectra for five of our six objects, none of which showed evidence for an active central region. Two of the spectra showed no strong emission lines, while two host galaxies (SDSS J084838.57+193528.9 and MRK 1097) showed star formation lines. It is possible that one or both of the galaxies for which we do not have optical spectra will turn out to be an AGN. Moreover, there are known cases of galaxies that seem consistent with an AGN model when observed in X-rays, but do not show evidence of nuclear activity in their optical spectra (Jackson et al. 2012). The details of the mechanism that hides the active region is still being disputed. While AGNs are known to exhibit variability, both on long and short timescales, the majority of this variability is low amplitude. For example, Saxton et al. (2011) found that, in a sample of over 1000 AGNs observed with both the *XMM-Newton* Slew Survey and RASS, only 5% varied by more than a factor of 10. Given the relative rarity of large amplitude variability in AGNs, and the current difficulty in describing optically quiescent but X-ray luminous galaxies, a low redshift, variable, “hidden” AGN might be an interesting source for future study.

#### 4.5. Spurious Detections

Given that we have selected objects that appeared in XMMSL1, but not in RASS, one has to consider the possibility that these are spurious detections, or perhaps that they are real sources, but the galactic associations are incorrect. We note that XMMSL1 is estimated to contain less than 1% false sources in the soft band (Saxton et al. 2008), though the stronger argument is that the associations with host galaxies are unlikely to all be false. To make a conservative estimate of the chance of false coincidences, we assumed a  $30''$  match radius, and imagined spreading the 94 objects in our sample with flux ratio greater than 10 randomly across the sky, so that there were  $1.7 \times 10^{-3}$  transient objects  $\text{deg}^{-2}$ . We found that the odds of finding the observed number of coincidences by chance were very small. For example, within 200 Mpc there are  $\sim 150,000$  known galaxies ( $3.6 \text{ galaxies deg}^{-2}$ ) (Kasliwal 2011). So, within 200 Mpc, our search had a 7% chance of finding even a single coincidence by chance, where we found four. Moreover, all but one of the sources matched their host galaxies within  $15''$  despite a  $30''$  search radius, and none of the transients were spatially inconsistent with having originated from within their hosts’ angular extent (see Table 2). For these reasons, most or all of the claimed galaxy associations are very likely real. It is worth noting, however, that one object has a slightly larger offset from the host galaxy, namely J202320.7–670021. The matched host galaxy is at a distance of only 67 Mpc, and the angular extent of the galaxy overlaps the  $1\sigma$  error circle from XMMSL1. So, while it seems likely that this association is real, in this case we are unable to rule out a spurious association.



## 5. CONCLUSIONS

In this work, we took a census of X-ray transient objects in the low redshift universe, motivated by future observations of compact object mergers with Advanced LIGO and Advanced Virgo. A wide-field, soft X-ray monitor such as the proposed ISS-Lobster will be able to seek counterparts to LIGO/Virgo events, but high-confidence identifications will demand high quality variability studies. We performed a systematic search for low-redshift, extragalactic transients in the *XMM-Newton* slew survey, covering 32,800 deg<sup>2</sup>, above fluxes of  $3 \times 10^{-12}$  erg cm<sup>-2</sup> s<sup>-1</sup> in the 0.2–2 keV band. We compared observations taken many years apart in the RASS and the XMMSL1, and found that over these long timescales, variations in flux divided sources into two categories: continuum variability, which can be described as a log-normal distribution in flux variability with a width of around 3, and state-change variability, corresponding to objects which show more dramatic changes in flux. State-change sources at low redshift may be confusion sources for future searches for counterparts to events measured with Advanced LIGO and Advanced Virgo, so we sought to characterize their density on the sky. We found that transient sources represented around 10% of all objects in a flux limited survey, and that of these, around 10% could be associated with known optical galaxies. For searches for LIGO/Virgo counterparts using wide-field X-ray imagers capable of observing hundreds of square degrees, we should expect around one false coincidence for every 10,000 deg<sup>2</sup> searched to a flux limit of  $10^{-11}$  erg s<sup>-1</sup> cm<sup>-2</sup>.

We found 12 objects meeting our search criteria, most of which were located within 350 Mpc. Of these, we identified six with clear galaxy identifications that were difficult to characterize and that have not been previously studied. They were highly luminous, highly variable, and lacked classical AGN optical signatures in the five cases with available spectra. Four of the sources (XMMSL1 J131951.9+225957, J084837.9+193537, J182609.9+545005, and J152408.6+705533) met all of the criteria of Esquej et al. (2007) for identifying candidate TDEs. One other seemed consistent with a TDE description, but may prove to be a variable AGN, and the sixth source had a measured position only marginally consistent with the center of the apparent host galaxy. It is possible that, whatever the nature of these sources, they represent some of the closest members of the class of unexplained, extragalactic transients identified by Starling et al. (2011), who focused on transient objects *not* associated with known galaxies. This study represents the first attempt to characterize soft X-ray confusion sources for counterparts to Advanced LIGO/Virgo merger events, and in the process, has revealed a handful of unusual objects that are both powerful and dynamic.

The authors are grateful for helpful discussions with Suvi Gezari, Judith Racusin, Brennan Hughey, Tracy Huard, and Sjoert van Velzan. We thank the anonymous referee for helpful comments. J.K. and L.B. were supported by appointments to the NASA Postdoctoral Program at GSFC, administered by Oak Ridge Associated Universities through a contract with NASA. K.M. would like to thank Branimir Sesar, Eric Bellm, and Yi Cao for help obtaining the P200 spectra, and Assaf Horesh for work with the Keck Observatory.

This research has made use of the NASA/IPAC Extragalactic Database (NED) which is operated by the Jet Propulsion Laboratory, California Institute of Technology, under contract

with the National Aeronautics and Space Administration. This research has made use of data obtained from the High Energy Astrophysics Science Archive Research Center (HEASARC), provided by NASA's Goddard Space Flight Center.

Funding for the SDSS and SDSS-II has been provided by the Alfred P. Sloan Foundation, the Participating Institutions, the National Science Foundation, the U.S. Department of Energy, the National Aeronautics and Space Administration, the Japanese Monbukagakusho, the Max Planck Society, and the Higher Education Funding Council for England. The SDSS Web site is <http://www.sdss.org/>.

The SDSS is managed by the Astrophysical Research Consortium for the Participating Institutions. The Participating Institutions are the American Museum of Natural History, Astrophysical Institute Potsdam, University of Basel, University of Cambridge, Case Western Reserve University, University of Chicago, Drexel University, Fermilab, the Institute for Advanced Study, the Japan Participation Group, Johns Hopkins University, the Joint Institute for Nuclear Astrophysics, the Kavli Institute for Particle Astrophysics and Cosmology, the Korean Scientist Group, the Chinese Academy of Sciences (LAMOST), Los Alamos National Laboratory, the Max-Planck-Institute for Astronomy (MPIA), the Max-Planck-Institute for Astrophysics (MPA), New Mexico State University, Ohio State University, University of Pittsburgh, University of Portsmouth, Princeton University, the United States Naval Observatory, and the University of Washington.

## REFERENCES

- Abadie, J., Abbott, B. P., Abbott, R., et al. 2012, *A&A*, **539**, A124
- Abadie, J., Abbott, B. P., Abbott, R., et al. 2010, *CQGra*, **27**, 173001
- Acernese, F., Alshourbagy, M., Amico, P., et al. 2008, *CQGra*, **25**, 184001
- Bade, N., Komossa, S., & Dahlem, M. 1996, *A&A*, **309**, L35
- Belczynski, K., Perna, R., Bulik, T., et al. 2006, *ApJ*, **648**, 1110
- Berger, E. 2010, *ApJ*, **722**, 1946
- Bhat, N. D. R., Chengalur, J. N., Cox, P. J., et al. 2013, *ApJS*, **206**, 2
- Bloom, J. S., Giannios, D., Metzger, B. D., et al. 2011, *Sci*, **333**, 203
- Bloom, J. S., Holz, D. E., Hughes, S. A., et al. 2009, arXiv:0902.1527
- Bloom, J. S., Richards, J. W., Nugent, P. E., et al. 2012, *PASP*, **124**, 1175
- Bloom, J. S., Sigurdsson, S., & Pols, O. R. 1999, *MNRAS*, **305**, 763
- Brandt, N., & Podsiadlowski, P. 1995, *MNRAS*, **274**, 461
- Burrows, D. N., Kennea, J. A., Ghisellini, G., et al. 2011, *Nat*, **476**, 421
- Camp, J., Barthelmy, S. D., Blackburn, L., et al. 2013, arXiv:1304.3705
- Cenko, S. B., Krimm, H. A., Horesh, A., et al. 2012, *ApJ*, **753**, 77
- Cenko, S. B., Kulkarni, S. R., Horesh, A., et al. 2013, *ApJ*, **769**, 130
- Chapman, R., Tanvir, N. R., Priddey, R. S., & Levan, A. J. 2007, *MNRAS*, **382**, L21
- Cobb, B. E., Bailyn, C. D., van Dokkum, P. G., & Natarajan, P. 2006, *ApJL*, **645**, L113
- Connors, A., Serlemitsos, P. J., & Swank, J. H. 1986, *ApJ*, **303**, 769
- Coward, D. M., Howell, E. J., Piran, T., et al. 2012, *MNRAS*, **425**, 2668
- Drake, A. J., Djorgovski, S. G., Mahabal, A., et al. 2011, *ApJ*, **735**, 106
- Eichler, D., Livio, M., Piran, T., & Schramm, D. N. 1989, *Natur*, **340**, 126
- Esquej, P., Saxton, R. D., Freyberg, M. J., et al. 2007, *A&A*, **462**, L49
- Esquej, P., Saxton, R. D., Komossa, S., et al. 2008, *A&A*, **489**, 543
- Evans, P. A., Fridriksson, J. K., Gehrels, N., et al. 2012, *ApJS*, **203**, 28
- Fairhurst, S. 2009, *NJPh*, **11**, 123006
- Fox, D. B., Frail, D. A., Price, P. A., et al. 2005, *Natur*, **437**, 845
- Fryer, C. L., & Kalogera, V. 1997, *ApJ*, **489**, 244
- Fryer, C. L., Woosley, S. E., & Hartmann, D. H. 1999, *ApJ*, **526**, 152
- Fuhrmeister, B., & Schmitt, J. H. M. M. 2003, *A&A*, **403**, 247
- Gao, H., Ding, X., Wu, X.-F., Zhang, B., & Dai, Z.-G. 2013, *ApJ*, **771**, 86
- Gezari, S., Chornock, R., Rest, A., et al. 2012, *Natur*, **485**, 217
- Gezari, S., Martin, D. C., Milliard, B., et al. 2006, *ApJL*, **653**, L25
- Gothelf, E. V., Hamilton, T. T., & Helfand, D. J. 1996, *ApJ*, **466**, 779
- Greiner, J., Hartmann, D. H., Voges, W., et al. 2000a, *A&A*, **353**, 998
- Greiner, J., Schwarz, R., Zharikov, S., & Orlo, M. 2000b, *A&A*, **362**, L25
- Grupe, D., Thomas, H.-C., & Leighly, K. M. 1999, *A&A*, **350**, L31
- Harry, G. M., et al. (LIGO Scientific Collaboration) 2010, *CQGra*, **27**, 084006
- Huang, Y. F., Dai, Z. G., & Lu, T. 2002, *MNRAS*, **332**, 735



- Jackson, F. E., Roberts, T. P., Alexander, D. M., et al. 2012, *MNRAS*, **422**, 2
- Kanner, J., Camp, J., Racusin, J., Gehrels, N., & White, D. 2012, *ApJ*, **759**, 22
- Kasliwal, M. M. 2011, PhD thesis, California Institute of Technology
- Kelley, L. Z., Ramirez-Ruiz, E., Zemp, M., Diemand, J., & Mandel, I. 2010, *ApJL*, **725**, L91
- Klimenko, S., Vedovato, G., Drago, M., et al. 2011, *PhRvD*, **83**, 102001
- Komossa, S., & Bade, N. 1999, *A&A*, **343**, 775
- Komossa, S., & Greiner, J. 1999, *A&A*, **349**, L45
- Kulkarni, S., & Kasliwal, M. M. 2009, in *Astrophysics e-prints*, Vol. 2010, astro2010: The Astronomy and Astrophysics Decadal Survey, [http://sites.nationalacademies.org/BPA/BPA\\_050603](http://sites.nationalacademies.org/BPA/BPA_050603)
- Lazio, J., Keating, K., Jenet, F. A., et al. 2012, in *IAU Symp. 285*, New Horizons in Time-domain Astronomy, ed. E. Griffin, R. Hanisch, & R. Seaman (Cambridge: Cambridge Univ. Press), 67
- Levan, A. J., Tanvir, N. R., Cenko, S. B., et al. 2011, *Sci*, **333**, 199
- Lin, D., Carrasco, E. R., Grupe, D., et al. 2011, *ApJ*, **738**, 52
- Maksym, W. P., Ulmer, M. P., & Eracleous, M. 2010, *ApJ*, **722**, 1035
- Matsuoka, M., Kawasaki, K., Ueno, S., et al. 2009, *PASJ*, **61**, 999
- Metzger, B. D., Kaplan, D. L., & Berger, E. 2013, *ApJ*, **764**, 149
- Metzger, B. D., Quataert, E., & Thompson, T. A. 2008, *MNRAS*, **385**, 1455
- Nakar, E. 2007, *PhR*, **442**, 166
- Nissanke, S., Kasliwal, M., & Georgieva, A. 2013, *ApJ*, **767**, 124
- Osborne, J. P., O'Brien, P., Evans, P., et al. 2013, arXiv:1302.2542
- Phinney, E. S. 2009, in *Astrophysics e-prints*, Vol. 2010, astro2010: The Astronomy and Astrophysics Decadal Survey, arXiv:0903.0098
- Predoi, V., Clark, J., Creighton, T., et al. 2010, *CQGra*, **27**, 084018
- Racusin, J. L., Liang, E. W., Burrows, D. N., et al. 2009, *ApJ*, **698**, 43
- Rhoads, J. E. 2003, *ApJ*, **591**, 1097
- Saxton, R. D., Read, A. M., Esquej, P., Miniutti, G., & Alvarez, E. 2011, in *Proc. Narrow-Line Seyfert 1 Galaxies and their Place in the Universe*, ed. L. Foschini et al. (Trieste: SISSA), *PoS(NLS1)008*
- Saxton, R. D., Read, A. M., Esquej, P., et al. 2008, *A&A*, **480**, 611
- Saxton, R. D., Read, A. M., Esquej, P., et al. 2012, *A&A*, **541**, A106
- Soderberg, A. M., Kulkarni, S. R., Nakar, E., et al. 2006, *Natur*, **442**, 1014
- Stappers, B. W., Hessels, J. W. T., Alexov, A., et al. 2011, *A&A*, **530**, A80
- Starling, R. L. C., Evans, P. A., Read, A. M., et al. 2011, *MNRAS*, **412**, 1853
- van Velzen, S., Farrar, G. R., Gezari, S., et al. 2011, *ApJ*, **741**, 73
- Veilleux, S., & Osterbrock, D. E. 1987, *ApJS*, **63**, 295
- Voges, W., Aschenbach, B., Boller, T., et al. 1999, *A&A*, **349**, 389
- Wang, J., & Merritt, D. 2004, *ApJ*, **600**, 149
- Winter, L. M., Mushotzky, R. F., & Reynolds, C. S. 2006, *ApJ*, **649**, 730
- Wright, E. L., Eisenhardt, P. R. M., Mainzer, A. K., et al. 2010, *AJ*, **140**, 1868
- Zhang, B. 2013, *ApJL*, **763**, L22